Classification of a Volumetric MRI Using Gibbs Distributions and a Line Model

Junchul Chun[1], Soo Il Kwon[2]

Purpose : This paper introduces a new three dimensional Magnetic Resonance Image classification which is based on Markov Random Field-Gibbs Random Field with a line model.

Material and Methods : The performance of the Gibbs Classifier over a statistically heterogeneous image can be improved if the local stationary regions in the image are disassociated from each other through the mechanism of the interaction parameters defined at the local neighborhood level. This usually involves the construction of a line model for the image. In this paper we construct a line model for multisignature images based on the differential of the image which can provide an a priori estimate of the unobservable line field, which may lie in regions with significantly different statistics. The line model estimated from the original image data can in turn be used to alter the values of the interaction parameters of the Gibbs Classifier.

Results : MRF-Gibbs classifier for volumetric MR images is developed under the condition that the domain of the image classification is E^3 space rather than the conventional E^2 space. Compared to context free classification, MRF-Gibbs classifier performed better in homogeneous and along boundaries since contextual information is used during the classification.

Conclusion : We construct a line model for multisignature, multidimensional image and derive the interaction parameter for determining the energy function of MRF-Gibbs classifier.

Index words : Markov Random Field ; Gibbs Random Field ; Line Model
Gibbs Classifier ; Volumetric MRI

Introduction

For the visualization or quantitative analysis of normal or abnormal soft tissue in MRI, proper classification of soft tissues is needed. In MRI the gray-level distributions between different soft tissues are not widely distributed and even more the complexity of tissue boundaries cause many pixels to contain mixtures of tissues. It is well-known that it is possible to obtain multiple images, so-called multi-echo images of same anatomical section of the human body using different pulse sequence in Magnetic Resonance Imaging(1,2). Each image has a different

JKSMRM 2 : 58-66(1998)
[1]Department of Computer Science, Imaging & Graphics Lab., Kyonggi University
[2]Department of Medical Physics, Kyonggi University
Received April 1, 1998 ; revised May 27, 1998 ; accepted June 22, 1998
Address reprint requests to : Junchul Chun, Department of Computer Science, Kyonggi University, Suwon, Korea.
Tel. 82-331-249-9668 Fax. 82-331-253-1165 Email. jcchun@kuic.kyonggi.ac.kr

response characteristic to each soft tissue class, thus this property of MRI and analysis of multiple image provide the potential for improving the accuracy of tissue classification(3, 4, 5).

The Gibbs Classifier is a discrete optimizing classifier which assign the image location x with observed image intensities $f(x)$ to the class ω_i by estimating the Maximum A Posteriori(MAP) estimate of the class distribution of the image(6, 7).

Gibbs classifier perform this task by equating the Markovian structure of the image with an equivalent Gibbs distributional structure. Thus this simplifies the problem of estimating all of the conditionals needed by the Markovian model by replacing that estimation problem with much simpler problem of estimating the parameters of a variety of potential functions which are identified with local neighborhoods of each image site. A common model for defining such potential functions involves the construction of interaction parameters i.e., a family of parameters which serve to indicate the relative strength of a neighboring site's contribution to the classification of the site under consideration.

In this paper, we present a computationally inexpensive, novel approach for the classification of volumetric multisignature Magnetic Resonance images. A statistical volumetric image model based on the Markov Random Filed and Gibbs Random Field model and an algorithm for the classification of the image will be pursued. To estimate the interaction parameter of the potential functions, we construct an unobservable line field, to be estimated from the original data, which can in turn be used to alter the values of the interaction parameters if it is thought that a particular clique is transected by a line. This is just the exchange of one difficult problem : classification for another : edge detection(8).

Theory and Method

1) MRF-Gibbs Model

The main idea of the MRF-Gibbs classification algorithm lies the Markov Random Field(MRF) assumption, which states that the true interpretation of any pixel X_{ij}, given the true interpretation of all image pixels depends only on the interpretation of its neighboring pixels in a neighborhood N_{ij}.

$$P(X_{ij}=\omega_k \mid G)=P(X_{ij}=\omega_k \mid N_{ij}) \qquad [1]$$

This interpretation of a pixel can be used for the assignment, or classification of a pixel to a class ω_k, which represents a labeling of the pixel from a given set N_{ij} of L possible classes. These classes may correspond to tissue types of the MRI. If N_{ij} is a four pixel neighbor-hood, the assignment of pixel N_{ij} to a class ω_k can be evaluated in terms of the posterior probability $P(\omega_k \mid X_{ij}, Q)$ the conditional probability that the assignment of class ω_k is correct given observation X_{ij} and prior information Q. From MRF assumption, the best classification for X_{ij} is the class ω_k that maximizes equation[2].

$$P(\omega_k)P(\bigcap_{(xy)\in N_i} \mid \omega_k) \geq P(\omega_h)P(\bigcap_{(xy)\in N_i} X_{xy} \mid \omega_h), \quad \forall\, h \neq k \qquad [2]$$

The MRF-Gibbs equivalence shows that the decision rule, defined above, can be written in a following Gibbsian form,

$$P(X_{ij}=\omega_k)=\frac{1}{Z}e^{-U(X_{ij},\,\omega_k)/T},$$
$$P(X_{ij}, \omega_k)=-\sum_{(xy)\in N_{ij}} \log P(X_{xy} \mid \omega_k)+U(\omega_k) \qquad [3]$$

and that this Gibbsian equivalent can be evaluated using an energy function, $U(X_{ij}, \omega_k)$. The MRF-Gibbs classification process consists of assigning the pixels of an image those class values which produce a maximum posterior distribution when the energy is minimized. Therefore, maximization of the posterior distribution for ta fixed X_{ij} is determined by minimizing the energy function $U(X_{ij}, \omega_k)$. As an approximate solution to this maximization problem can be solved using simulated annealing.

2) A Line Model for Gibbs Classifier

The derivation of energy function typically involves understanding the nature of the image, identifying a meaningful neighborhood shape, and describing the unique attributes of the image regions or structure. In this section, we construct an edge model for multisignature, multidimensional image and derive the Gibbs interaction parameter for determining the energy function. A multisignature volumetric MR image can be considered as a map

$$f : U \subset R^3 \rightarrow F \subset R^n$$

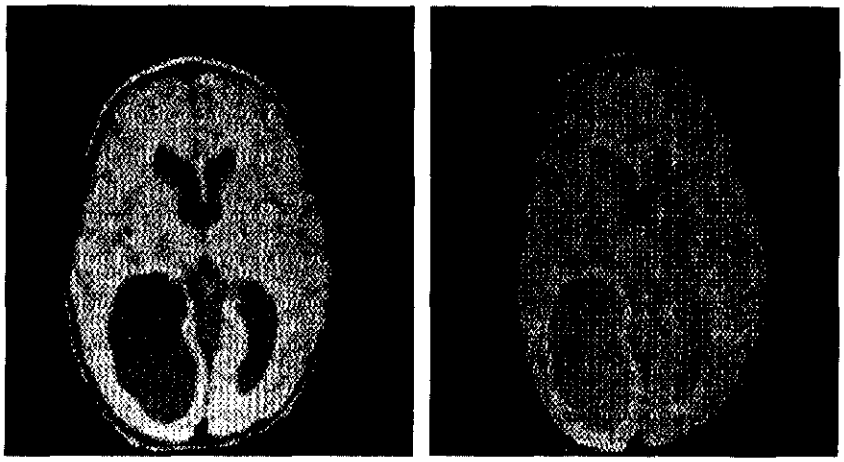

Fig. 1. Echoes 1 and 2

where U is the image domain and n is the spectral dimension of the image. One conventionally thinks of F as the unit hypercube in R^n. Most modern multisignature MR images aries from multiecho imaging techniques, and n=2 is the spectral dimension that we deal with in this paper. Fig. 1 shows both echoes taken from a midbrain slice of a patient with significant hydrocephalus.

The bulk of this section is a restatement of elementary results in differential geometry(9, 10). Suppose E and F are two normed vector spaces, and let L(E,F) be the space of continuous linear maps from E to F. Throughout the following U is taken to be open. Then the function(image), $f:U \subset E \rightarrow F$, is differentiable at u_L:U if there is an $L \in L(E, F)$ such that the map g_L:$U \in E \rightarrow F$ defined by $g_1(u): f(u_0) + L(u-u_0)$ is tangent to f at u_0. Then one defines the derivative of f at u_0 to be $df(u_0)=L$. When $U \subset R^n$ and $f:U \rightarrow R^m$ is differentiable, then the linear map $df(x)$ has the common expression in terms of the Jacobian matrix with respect to the standard bases of R^n and R^m, given by

$$df(x) = \begin{vmatrix} \frac{\partial f^1}{\partial x^1} & \frac{\partial f^{f1}}{\partial x^2} & \cdots & \frac{\partial f^1}{\partial x^n} \\ \frac{\partial f^2}{\partial x^1} & \frac{\partial f^2}{\partial x^2} & \cdots & \frac{\partial f^2}{\partial x^n} \\ & \cdots\cdots\cdots & & \\ \frac{\partial f^m}{\partial x^1} & \frac{\partial f^m}{\partial x^2} & \cdots & \frac{\partial f^m}{\partial x^n} \end{vmatrix} \quad [4]$$

where it is understood that the partials are evaluated at $x=(x^1, x^2, x^3, \ldots x^n)$. We denote the evaluation of $df(x)$ on $e \in E$ by $df(x) \cdot e$.

If $f:U \subset E \rightarrow F$; the f has a derivative in the direction $e \in E$ at $u \in U$ provided

$$\frac{d}{dt} f(u+te) \mid_{t=0} \quad [5]$$

exists. If f is differentiable, then the directional derivatives of f all exist at u and are given by

$$\frac{d}{dt} f(u+te) \mid_{t=0} = df(u) \cdot e \quad [6]$$

This leads to a strategy for characterizing the map which we call the max norm characterization; we set $\mu(f(u))=e_0$ where $e_0 \in E$ satisfies

$$\mid df(u) \cdot e_0 \mid_2 = \max_{e \in E: \mid e \mid_2=1} \mid df(u) \cdot e \mid_2 \quad [7]$$

In the simplest meaningful case ($E=F=R^2$), e_0 is one of the π periodic extension of $e=(\sin\theta, \cos\theta)$. In higher dimension it may be necessary to resort to a numerical strategy determine $\mu(f(u))$. We will use the distribution of the 2-norm

$$\mid \mu(f(u)) \mid_2 = \mid df(u) \cdot e_0 \mid_2 \quad [8]$$

as a means of determining the relative strength of map $df(u)$. We have observed that a not unreasonable fit to the distribution of $\mid \mu(f(u)) \mid_2$ can be given by the Rayleigh distribution $R(\sigma)$ with σ set to the mode of $\mid \mu(f(u)) \mid_2$.

Let $R(x, \sigma)$ be the Rayleigh distribution function with parameter σ; then we define the edge probability under df to be the random variable

$$p_u(e_0)=R(|\mu(f(u))|_2;m(|\mu(f(u))|_2)) \quad [9]$$

where m is taken to be the mode. As defined in the usual way in the Gibbs paradigm suppose $u \in E$ is a site with neighbors $\{u_1, u_2, \cdots, u_m\}$ and let $\{\beta_1, \beta_2, \cdots, \beta_m\}$ be the interaction parameters between u and its neighbors such that $-\alpha \leq \beta_i \leq \alpha$. Whenever β_i is positive, u and u_i are statically more likely to arise from the same underlying class; whenever β_i is negative, u and u_i are less likely to arise from the same class. One simple assignment to the interaction parameters is to assign

$$\theta_i=h(\alpha(1-2p_u(e_0))) \quad [10]$$

to that u_i most proximal to the cardinal direction of e_0 to the u_i in the anti-cardinal direction and an interpolate between $-\theta_i$ and θ_i to the remaining sites depending on their proximity to $u+e_0$ or $u-e_0$. The function h in the equation (10) can be taken to be any function which maintains the intent of the interaction parameters. Two obvious candidates are the linear and cubic variations $h(\alpha(1-2p_u(e_0)))=\alpha(1-2p_u(e_0))$ and $h(\alpha(1-2p_u(e_0)))=\alpha(1-2p_u(e_0))^3$.

Experimental Results

MRF-Gibbs classifier for volumetric MR images is developed under the condition that the domain of the image classification is E^3 rather than the conventional E_2 space. The implementation of the MRF-Gibbs classifier was approach through a series of phase. The phases were, construction of a volumetric image, clustering analysis of such image, parameter estimation for the Gibbs energy function, and MRF-Gibbs re-classification iteration.

The first phase to prepare for the Gibbs classification of a volumetric image is to construct a volumetric image and analyze the volumetric data using any clustering analysis technique. In general, a volumetric MR image can be constructed from the slices of two dimensional images. In pur case, we adopt a computationally least expensive way of obtaining a volumetric image data which is stacking the slices of two dimensional images using interpolation between the original planes. The MR image given to us is a composite MR image (dual-echo slice). The typical dual-echo sequence involves 15 transverse imag-es taken through the human brain; each slice is 7 mm thick and the separation between two consecu-tive slices is 8.5 mm center to center on the Z-axis. Therefore, each image is a series of 15 geometric slices of images, consisting of SD and T2 image slices alternating one after another.

Since medical imaging modalities leave unimaged space between adjacent slices (8.5 mm in our case) of images, interpolation can be used to fill in the space between the slices. Interslice voxel values are estimated by computing a linear average of the density values found in pairs of opposing voxels in the original slices. Such a volumetric image is shown in Fig. 2.

Next phase is to derive the interaction parameters

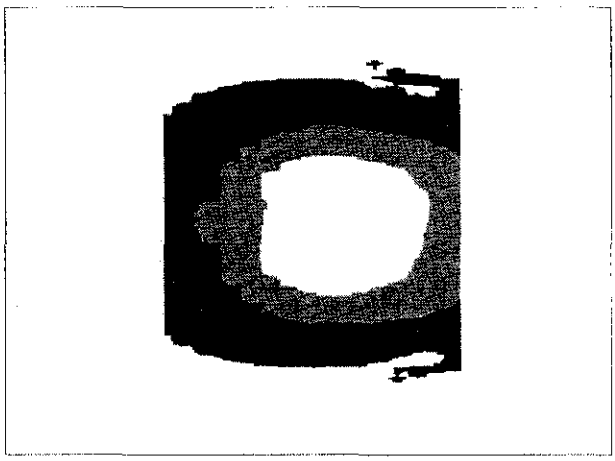

Fig. 2. Reconstructed Volumetric Magnetic Resonance Imagery

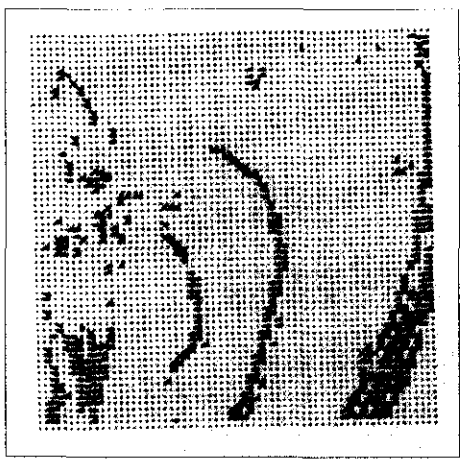

Fig. 3. Sample Vector Field, $\mu(f(u))$

for defining potential function of MRF-Gibbs classifier. As for the case of the two dimensional multisignature image, Fig. 3 shows a part of the planer vector field $\mu(f(u))$ of Fig. 1 showing the direc-tions in which planer interaction parameters would be set according to the description above. These parameters serve to indicate the relative strength of a neighboring site's contribution to the classification of the site under consideration.

In a higher dimensional case i.e., the volumetric multisignature image, the vector field can be reduced easily. Fig. 4 shows the surface corresponding to $| df(u) \cdot e(\theta, \phi) |_2$ for a fixed u, plotted as a function of the parameters (θ, ϕ) of the unit 3-vector $(\theta, \phi) = (\sin\theta\cos\phi, \sin\theta, \sin\phi, \cos\theta)$ fixed at u. It is a simple matter to locate the maxima of this surface. Once computed, the 3-space directional vector field $\mu(f(u))$ of a volumetric image is straightforward to construct. Fig. 5 shows such a vector field with maximizing and minimizing vector plotted.

The final phase, MRF-Gibbs iteration, involves the actual re-classifying of the pixels through a series of re-classification iterations. The Gibbs classifier developed has been applied to two dimensional MRI and volumetric MRI.

It is often necessary to generate a simulated data set prior to applying the developed classification algorithms to MRI, in order to evaluate the performance of the classifier, especially when we have no known class map information of the MRI. Therefore, we can generate multivariate synthetic images and evaluate the performance of the classifier against the test images.

The synthetic image which is illustrated in Fig. 6 (a) has four different distribution and each distribution is assigned to each quadrant of the image. The distribution of each quadrant of the image (numbered 1 to 4 from the left lower conner working counter clockwise) is normally distributed with the means M1=(60, 50), M2=(130, 120), M3=(220, 190), M4=(290, 270) and the covariances $\sigma_{11}=\sigma_{22}\sqrt{10000}$.

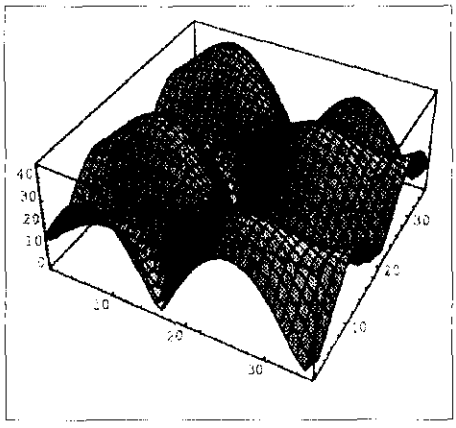

4

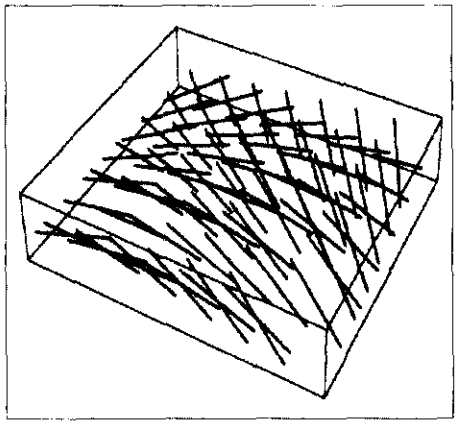

5

Fig. 4. $| df(u) \cdot e(\theta, \phi) |_2$

Fig. 5. Sample 3D Vector Field, $\mu(f(u))$

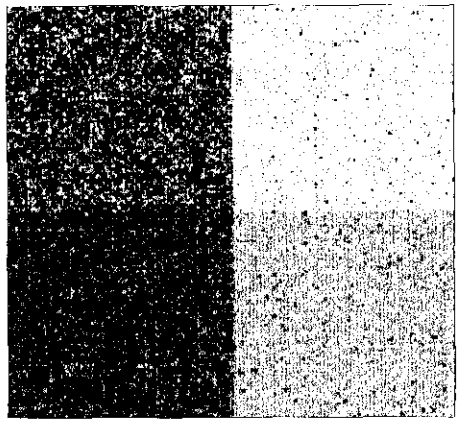

a

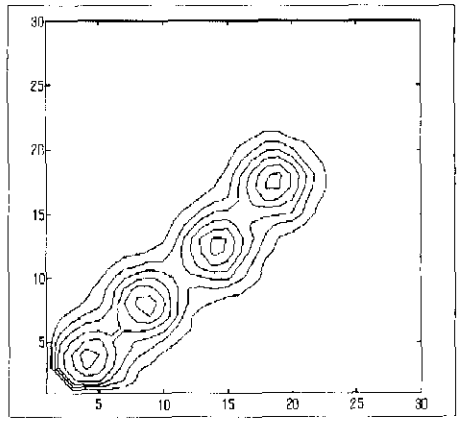

b

Fig. 6. (**a**) A Multivariate Synthetic Image (**b**) Cluster Distribution of Synthetic Image

As illustrated in Fig. 6(b) the natural groups of each distribution of the quadrant is overlapped each other and we consider each natural group as a cluster.

Fig. 7 shows various classification results based on context-free classification along with MRF-Gibbs classification. From the results of classification (Table 1—4) the error rate of 1st order MRF-Gibbs classification is much smaller (0.0045) than the results of context-free classification such as K-means classification, maximum likelihood estimation and Euclidean distance/Maximum likelihood classification with error rates 0.075, 0.0723 and 0.0701 respectively.

Classification

In the classification of a two dimensional MR image we performed context free classification i.e., maximum likelihood and minimum distance classification along with Gibbs classification. The class maps of such classification are shown in Fig. 8. Much of noise in the class maps based on context free classification are removed when we use Gibbs clas-

Table 1. Cluster Allocation to each Quadrant For K-Nearest Means Classification of Synthetic Image

Quadrant	Cluster 1	Cluster 2	Cluster 3	Cluster 4
1	15021	1363	0	0
2	925	14808	651	0
3	0	1064	14959	361
4	0	0	557	15827

Table 2. Cluster Allocation to each Quadrant For Maximum Likelihood Estimation of Synthetic Image

Quadrant	Cluster 1	Cluster 2	Cluster 3	Cluster 4
1	14981	1403	0	0
2	636	15201	547	0
3	0	634	15018	732
4	0	0	797	15587

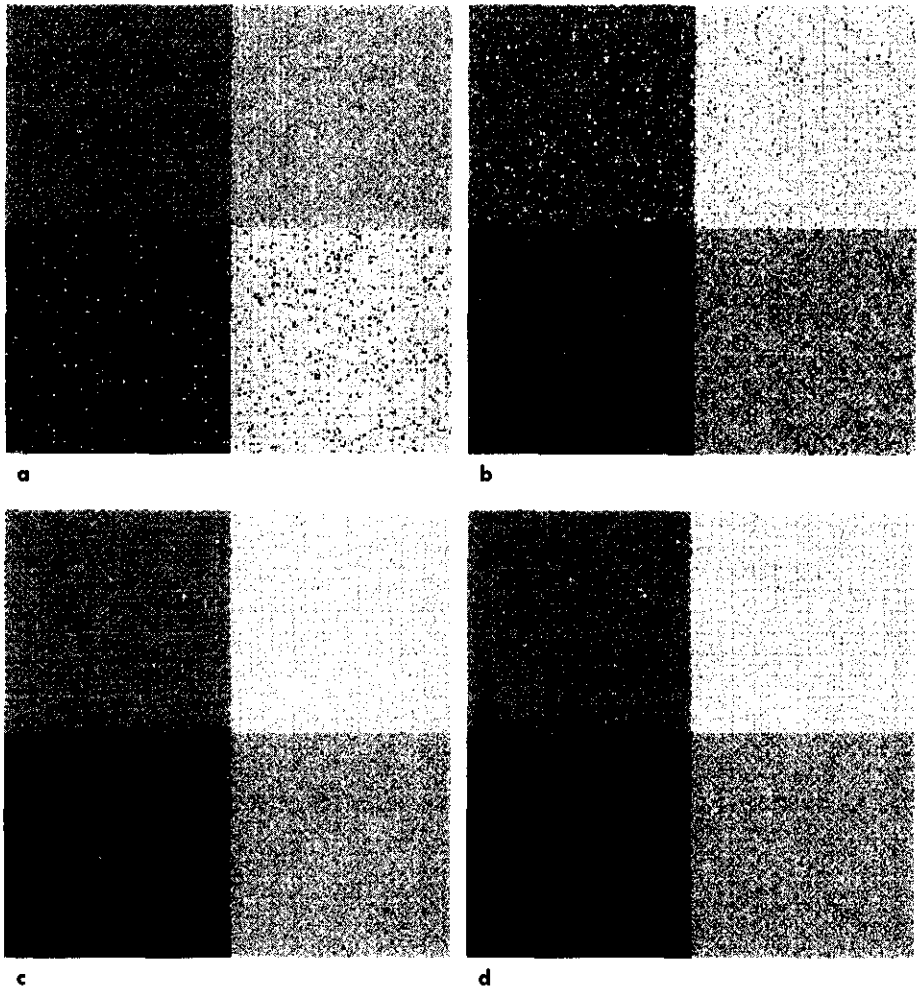

Fig. 7. Classification Results of Synthetic Image : (**a**) Maximum Likelihood Estimation, (**b**) Euclidean Distance/Maximum Likelihood Classification, (**c**) 2nd Order Gibbs Classification, (**d**) 1st Order Gibbs Classification.

classifier. Finally, Fig. 9 shows the Gibbs classification maps for partial volume of midbrain images reconstructed.

Discussion

This paper introduces MRF-Gibbs classifier using a line model for multi-spectral, and multidimensional images, i.e, volumetric multisignature Magnetic Resonance images. For this purpose, we expanded the domain of image classification from conventional two dimensional plane to three dimensional space. Then, a three dimensional Bayesian model is constructed based on the MRF-GRF stochastic model. Finally, a relaxation and annealing algorithm was used to obtain three dimensional MAP estimates of the volumetric multisignature images. In this paper, we have described the role of the total differential of a multisignature image in constructing a line model for such images, and in the setting of interaction parameters for an MRF-Gibbs classifier.

In practices, to lessen the computational burden

Table 3. Cluster Allocation to each Quadrant For Maximum Likelihood Classification with Euclidean Distance Clustering Criteria

Quadrant	Cluster 1	Cluster 2	Cluster 3	Cluster 4
1	15382	1002	0	0
2	878	14900	605	0
3	0	577	15009	798
4	0	0	749	15635

Table 4. Cluster Allocation to each Quadrant For 1st Order MRF-Gibbs

Quadrant	Cluster 1	Cluster 2	Cluster 3	Cluster 4
1	16338	46	0	0
2	73	16282	29	0
3	0	28	16282	74
4	0	0	26	16358

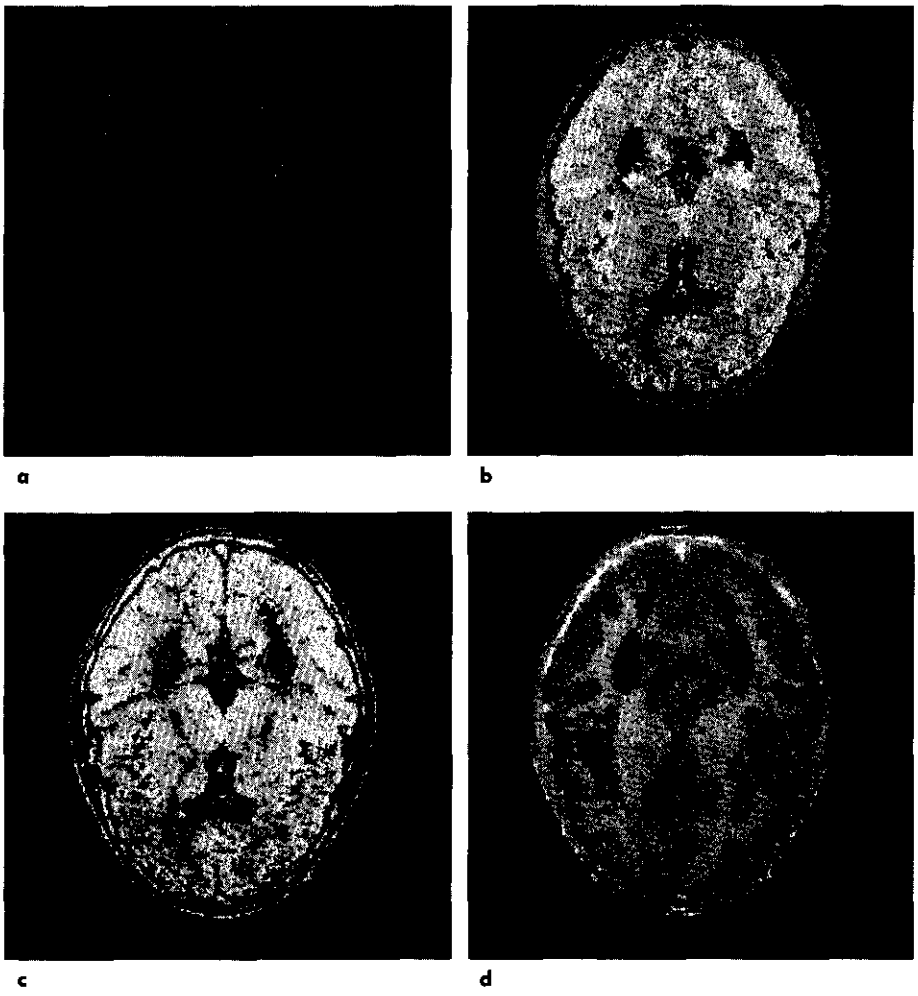

Fig. 8. a. A multi-Echo Magnetic Resonance Image.
b. Result of maximum likelihood classification.
c. Result of minimum distance classification (**d**) Result of Gibbs classification.

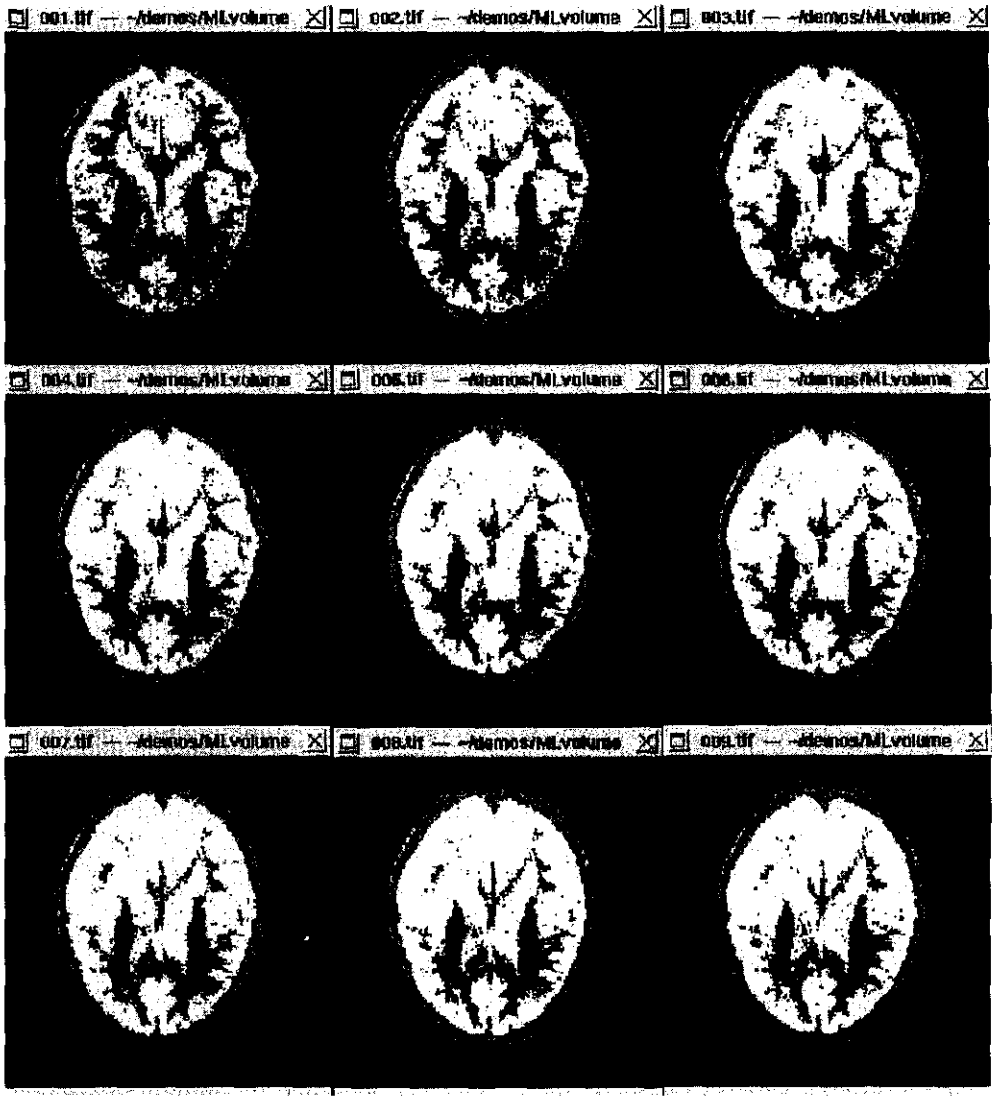

Fig. 9. Gibbs Classification Results of a Reconstructed Volumetric MRI

in the simulated annealing algorithm, we developed a parallel algorithm which ran on 12 processor Sparc Center 2000 system. Compared to context free classification, MRF-Gibbs classification performed better in homogeneous and along boundaries since contextual information is used during the classification. In evaluating the relative performance of the classifiers, we have used the subjective analysis of professional clinical scientists. The classification results will provide the clinically important data to analyze the abnormal tissue in the human brain. Moreover, the class maps generated from the volumetric image will allow us to visualize specific three dimensional tissue objects in the brain.

References

1. Elster AD. Magnetic Resonance Imaging: J.B. Lippincott Company, 1986
2. Bushong SC. Magnetic Resonance Imaging-Physical and Biological Principles: The C.V. Mosby Company, 1988
3. Santago P, Gage HD. Quantification of MR Brain Images by Mixture Density and Partial Volume Modeling. IEEE Trans. on Medical Imaging 1993;12:566-574
4. Choi HS, Haynor DR, Kim Y. Partial Volume Tissue Classification of Multichannel Magnetic Resonance Images-A Mixel Model. IEEE Trans. on Medical Imaging 1991;10:395-407
5. Taxt T, Lundervold A. Multispectral Analysis of the Brain Using Magnetic Resonance Imaging. IEEE Trans. on Medical Imaging 1994;13:470-481
6. Geman S, Geman D. Stochastic relaxation, Gibbs distributions, and Bayesian restoration of images. IEEE Trans. on

Pattern Anal. Mac. Intel 1994;6:721-741
7. Acuna C. Texture Modeling using Gibbs Distributions. CVGIP:Graphical Models and Image Processing 1992;6:210-222
8. Brummer ME, Mersereau RM, Eisner RL, Lewine RRJ. Automatic Detection of Brain Contours in MRI Data Sets. IEEE Trans. on Medical Imaging 1993;12:153-166
9. Abraham R, Marsden JE, Ratiu T. Manifolds, Tensor Anaysis, and Applications. New York:Springer-Verlag, 1988
10. Spivak M. Differential Geometry. (Vol. 1). MA:Publish or Perish, 1979

대한자기공명의과학회지 2:58-66(1998)

깁스분포와 라인모델을 이용한 3차원 자기공명영상의 분류

전 준 철, 권 수 일

경기대학교 기초과학 · 의학물리연구소

목 적 : 본 논문은 마코브 랜덤필드(Markov Random Field)와 깁스 랜덤필드(Gibbs Random Field) 및 라인모델(Line Model)에 기반한 3차원 자기공명영상의 분류 방법을 소개하고자 하였다.

대상 및 방법 : 통계학적으로 이질적 성분들로 구성된 영상을 대상으로한 깁스분류 결과는 영상내의 국소적으로 정적인 영역들을 이웃화소 시스템 내에서 정의되는 상호작용 인자(interaction parameter)의 메커니즘에 의해 분리함으로서 개선시킬 수 있다. 이를 위하여 영상에서 라인모델의 생성을 고려할 수 있으며, 본 논문에서는 영상의 미분방법에 근거한 다중신호영상을 위한 라인모델을 구축하였다. 라인모델은 서로 상이한 통계적 특성을 갖는 영역사이에 존재하는 관측할 수 없는 라인필드의 존재 유무를 확률 값으로 제공한다. 영상으로부터 획득한 라인모델은 Gibbs분류기의 에너지함수 값을 결정하는 상호작용 인자 값을 결정하는데 사용된다.

결 과 : 3차원 자기공명영상의 분류를 위한 MRS-Gibbs 분류기는 영상분류의 도메인이 일반적인 이차원 영상의 E^2 공간에서 E^3 공간으로 확장되었다. 개발된 깁스분류기를 이용한 자기공명영상의 분류결과 기존의 context free 분류방법에 의한 결과에 비하여 특히 동일성질을 갖고 있는 영역 및 경계부분 등의 분류결과가 우수함을 알 수 있었다.

결 론 : 본 논문에서는 다중신호, 3차원 자기공명영상을 위한 라인모델을 구축하고 그로부터 MRF-Gibbs 분류기의 에너지함수를 결정하기 위한 상호작용 인자를 유도하였다.

통신저자 : 전준철 경기도 수원시 팔달구 이의동 산 94-6 경기대학교 기초과학 · 의학물리연구소
Tel. 82-331-249-9668 Fax. 82-331-253-1165